

Performance Analysis of NB-Convolutional Coded OFDM on PLC Channel

Wael Abd-Alaziz, Martin Johnston

Abstract—Coded power line communication (PLC) promises significant enhancement to the overall system performance over uncoded PLC systems. Yet, there is limited contribution on the theoretical analysis of coded OFDM-PLC systems. In this letter, the β $\beta^2/1$ and $\beta^1\beta^1\beta^2/1$ NB-Convolutional (Non Binary) codes have been examined in an extreme PLC environment and an investigation of the performance analysis in terms of bit error rate (BER) of coded orthogonal frequency-division multiplexing (OFDM) PLC systems has been carried out. This analysis is accomplished with consideration of the realistic PLC frequency multi-path channels and for variant values of the background to impulsive noise ratio Γ . Finally, a fair comparison of the BER performance of β $\beta^2/1$ NB-convolutional code with $(1, 7/5)_8$ binary code is carried out.

Index Terms—NB-convolutional, GF(4), OFDM, PLC, Non-Gaussian, impulsive noise, Middleton class A.

I. INTRODUCTION

EXPLOITING the already established electrical grid does position PLC favorably, although the unsuitability of power line networks for communication services can make transmission quite unreliable because of vulnerability to attenuation, impulsive noise and the frequency-selective channels [1], [2]. In such extreme environments, error detection and correction techniques alone cannot cancel the serious impact of the channel and must be joined with the signal processing techniques such as channel estimation, channel equalization and OFDM, as we can see in [3]–[9]. These papers were showing the benefits of using coding channel on PLC systems, but there exists no validation of their results because they did not validate it theoretically and did not examine their proposed systems on realistic PLC channels. In this paper, good NB-convolutional codes [10] have been employed on OFDM-PLC system over practical PLC channels [11]. Additionally, the simulated and theoretical systems BER performance have been presented. In order to demonstrate the accuracy of our analysis, we have implemented and tested the results on three different binary and NB codes, where the MAX-Log-Map was used as a decoding algorithm [12]. To the best of the authors' knowledge, there is no research paper on the performance analysis of binary and NB-convolutional coded OFDM on PLC channel.

This letter is organized as follows: section II introduces the performance analysis of binary and NB-Convolutional Codes on Gaussian channel. While in section III, the performance analysis of coded binary and NB-Convolutional OFDM-PLC Systems has been investigated. Furthermore, in section IV, we present the simulated results of BER along with the

theoretical BER to illustrate the validation of the proposed analysis.

II. PERFORMANCE ANALYSIS OF BINARY AND NB-CONVOLUTIONAL CODES

It is well-known that the free distance of binary and NB-convolutional codes offer an approximated first order of the error performance. Therefore, the following equation is still valid on the matter of estimating the error performance of NB-convolutional codes

$$P_b \lesssim \sum_{w=d_{min}}^{\infty} c_w P_w, \quad (1)$$

where c_w is the number of codewords of weight w , P_w is the pairwise error probability, and it's given by [13]:

$$P_w = Q\left(\frac{d_E}{2\sigma}\right), \quad (2)$$

where, d_E is the Euclidean distance between the transmitted all zero codewords $m(0)$ and the received codewords $c(\hat{m})$. For binary codes on AWGN, $d_e = 4wE_s$, as we can see in [13]. While for NB $Gf(4)$ on AWGN channel, it can be evaluated as, let $m(0) = [(+\sqrt{E_s}, +\sqrt{E_s})]$, $m(1) = [(-\sqrt{E_s}, +\sqrt{E_s})]$, $m(\beta) = [(+\sqrt{E_s}, -\sqrt{E_s})]$ and $m(\beta^2) = [(-\sqrt{E_s}, -\sqrt{E_s})]$, where E_s is the average code-bit energy, it is related to the code rate R_c and the average data-bit energy E_b . It is calculated by $E_s = R_c E_b$. However, the Euclidean distance in this case is calculated as

$$d_E = \sqrt{(2\sqrt{wE_s})^2 + (2\sqrt{wE_s})^2 + (4\sqrt{wE_s})^2} = \sqrt{24wE_s} \quad (3)$$

since P_w is the probability that the noise on the decoder output has occurred and it is true only if the received signal has been affected by a noise magnitude greater than $d_E/q = \frac{\sqrt{24wE_s}}{4} = \sqrt{\frac{3wE_s}{2}}$. Now, the pairwise error probability can be evaluated by:

$$P_w(\text{binary}) = Q\left(\sqrt{\frac{2wE_s}{N_0}}\right) = Q\left(\sqrt{\frac{2wR_cE_b}{N_0}}\right) \quad (4)$$

$$P_w(\text{NB}) = Q\left(\sqrt{\frac{3wE_s}{N_0}}\right) = Q\left(\sqrt{\frac{3wR_cE_b}{N_0}}\right) \quad (5)$$

Thus, the probability of codeword error P_{cw} and the bit error probability P_e can be obtained from equations 4 and 5 as in [13],

$$P_e = \frac{1}{k} \sum_{w=d_{min}}^N T'_w P_w \quad (6)$$

where T'_w is the number of non-zero bits identical to all the codewords with a weight of w which is estimated with the help of the transfer function. Since driving a transfer

Wael Abd-Alaziz is a Lecturer at the College of Computer Science and Information Technology in the University of Sumer, e-mail: w.abdalaziz@uos.edu.iq.

Martin Johnston is a Senior Lecturer at the School of Engineering in Newcastle University, e-mail: martin.johnston@ncl.ac.uk.

function (TF) is too long a process, in this section, the authors will introduce only the outcome of NB TSs as examples to demonstrate the accuracy of the proposed analysis, while the derived TF of $\beta \beta^2/1$ code is carried out in the appendix along with their encoder block diagrams as shown in figures 9 and 10, respectively. The symbol TF of the NB $\beta \beta^2/1$ and $\beta 1\beta/1\beta^2$ codes, respectively are:

$$T'_w = 2W^3 + 8W^4 + 14W^5 \dots \quad (7)$$

$$T'_w = 5W^4 + 0W^5 + 33W^6 \dots \quad (8)$$

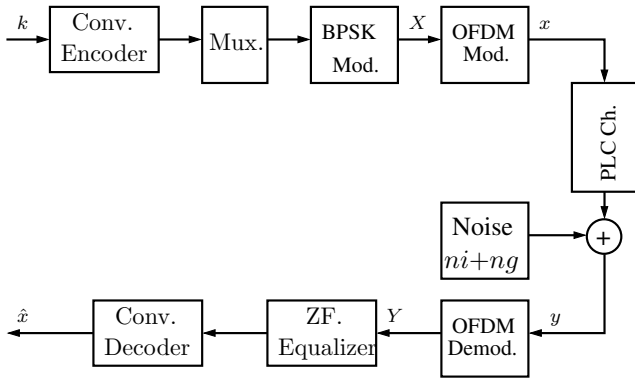


Fig. 1. Convolutional coded OFDM-PLC system diagram.

III. PERFORMANCE ANALYSIS OF CODED BINARY AND NB-CONVOLUTIONAL OFDM-PLC SYSTEMS

Figure 1 illustrates the block-diagram of a general convolutional coded OFDM-PLC system with ZF equalizer. Basically, a k length data will pass through a rate half convolutional encoder and then the output message and parity bits or symbols will be mixed into one stream of data. This stream will be mapped by BPSK mapper, IFFT will be applied to the mapper output and the resulting signal x will be transmitted via PLC channels. The received signal y at the receiver side can be estimated as:

$$y = h * x + n \quad (9)$$

where x is $[\pm 1]$ BPSK symbols, h is the multi-path frequency selective channel coefficients, n is the Middleton class A noise samples, and its PDF is defined as [1],

$$p(X) = \sum_{m=0}^{\infty} \frac{e^{-A} A^m}{m!} \cdot \frac{1}{\sqrt{2\pi\sigma_m^2}} \exp\left(-\frac{|X|^2}{2\sigma_m^2}\right), \quad (10)$$

where the variance σ_m^2 is given as

$$\sigma_m^2 = \sigma_u^2 \left(\frac{m}{A} + \Gamma \right) \quad (11)$$

and

$$\sigma_u^2 = \sigma_G^2 + \sigma_I^2, \quad \Gamma = \frac{\sigma_G^2}{\sigma_I^2}. \quad (12)$$

The parameters σ_G^2 and σ_I^2 are the variances of Gaussian noise and non-Gaussian noise (*i.e.* impulsive noise), respectively. Γ is the background to impulsive noise ratio parameter which marks the strength of the impulsivity as compared to Gaussian noise. A is the impulsive index which increases the impulsive behavior as it becomes larger. Furthermore, the

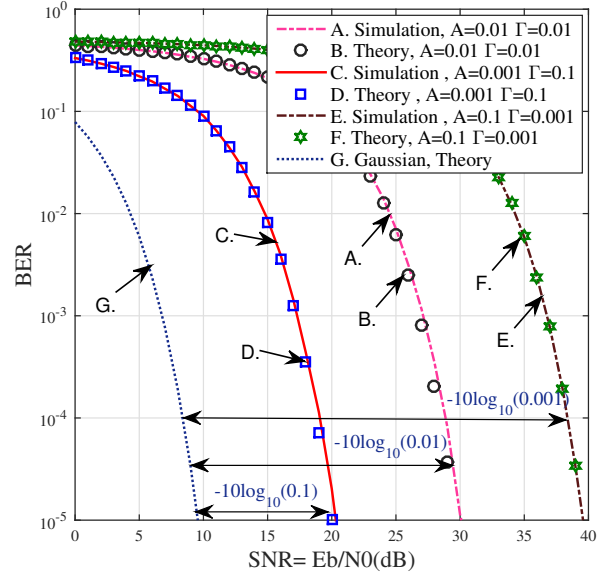


Fig. 2. Theoretical and simulated BER Performance of multi-carrier uncoded BPSK system on additive Middleton class A noise channel for variant values of A and Γ vs. SNR in dB.

total variance σ_z^2 of Middleton Class A noise of frequency domain can be approximated as a Gaussian distribution, but with a different variance $\mathcal{N}(0, \sigma_z)$ as evidenced by [3].

$$\sigma_z^2 = \frac{1}{N} \sum_{n=0}^{N-1} \sigma_z^2 = \sigma_G^2 \left(1 + \frac{1}{\Gamma} \right) \quad (13)$$

Figure 2 shows the idea of distributing the noise energy equally on every symbol and the BER curves will look like AWGN performance curves, but with different variance depending on the values of Middleton class A parameters (*i.e.* A and Γ). It is worth mentioning, as we can see on this figure, the value of A does not affect the performance of PLC systems that utilize OFDM.

Next, FFT will be applied to the received signal and then, ZF equalizer will be used to eliminate the multi-path frequency selective impact. Finally, the equalizer output will pass through Max-Log convolutional decoder to obtain \hat{x} .

However, according to [14], the probability of errors for uncoded system on AWGN and multi-path channels environment can be bounded by

$$P_e = Q\left(\sqrt{2\gamma_b}\right) \quad (14)$$

where γ_b is the SNR per bit and it is evaluated as

$$\gamma_b = \frac{Eb}{2\sigma_G^2} \sum_{n=1}^K |h(n)|^2 \quad (15)$$

where K is the length of the transmitted waveforms. After this preface and with help of OFDM, equation 14 can be considered for Middleton class A noise channel on frequency selective Rayleigh fading channel by substituting σ_z in equation 13 into equation 15.

Again, by using the same procedure of the uncoded systems, the performance analysis of coded binary and NB-convolutional OFDM-PLC systems can be accomplished. In

other words, the pairwise error probability P_w of convolutional codes in equations 4 and 5 will be written respectively as,

$$P_w(\text{binary}) = \frac{1}{K} \sum_{n=1}^K Q \left(\sqrt{\frac{wR_c E_b}{\sigma_z^2}} \right) \quad (16)$$

$$P_w(\text{NB}) = \frac{1}{K} \sum_{n=1}^K Q \left(\sqrt{\frac{3wR_c E_b}{2\sigma_z^2}} \right) \quad (17)$$

By submitting the new P_w for both codes into equation 6, the probability of error P_e can be estimated.

IV. SIMULATION RESULTS

In this section, we will present a comparison between the simulated and theoretical BER performance of binary and NB coded convolutional OFDM-PLC systems. The message length for the $(1, 7/5)_8$ binary code has been set to 2048 bits, and for the NB codes has been set to 1024 symbols. The rustles have been extracted for $A=0.1$, variant values of Γ s, and for two different multi-path channels that were introduced in [11].

As for authenticating this paper's assumption, in addition to evaluating the precision of the equations (13, 16 and 17), the following systems have been applied which are illustrated in figures 3 and 4: binary and non-binary convolutional coded OFDM on impulsive noise.

Figure 3 illustrates the simulation and theoretical BER of the $(1, 7/5)_8$ binary and $\beta_1\beta/\beta^2/1$ non-binary convolutional codes, while figure 4 shows the performance analysis of $\beta\beta^2/1$ non-binary convolutional code. Both figures show a good agreement between the simulation and the theoretical results for different values of Γ . This concurrence indicates an acceptable level of alignment between the practical and theoretical systems, ensuring and verifying the accuracy of the derived equations.

Figure 5 compares the analytical results with the simulated results of coded $(1, 7/5)_8$ binary and $\beta_1\beta/\beta^2/1$ NB for several values of Γ over 4 multi-path channel. This figure shows an excellent accord between the analytical and the simulated results.

Moreover, figure 6 depicts the performance of the same systems as figure 5 for numerous Γ values over a real-world 15 multi-path channel model. Evidently, figure 6 is displaying the precision of the performance analysis of coded OFDM-PLC system, whilst the channel is in extremely harsh condition, as well.

That is to say, figures 5 and 6 signify BER of coded $(1, 7/5)_8$ binary and $\beta_1\beta/\beta^2/1$ NB-convolutional OFDM-PLC systems over 4 and 15 multi-path channel models, respectively. The aforementioned figures have shown a very tight performance bound in each and every case, confirming the accuracy of the mentioned equations.

Finally, Figure 7 indicates the performance analysis of coded $\beta\beta^2/1$ NB-convolutional OFDM-PLC system across various realistic PLC channel models. As can be observed, there is acceptable correspondence between the theoretical and simulated findings.

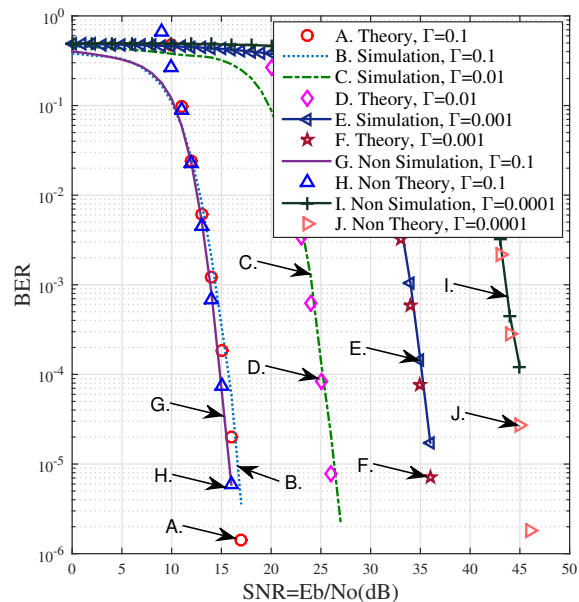


Fig. 3. Theoretical and simulation BER Performance of multi-carrier $(1, 7/5)_8$ binary and $\beta_1\beta/\beta^2/1$ non-binary convolutional codes on additive Middleton class A noise channel for different values of A and Γ vs. SNR in dB.

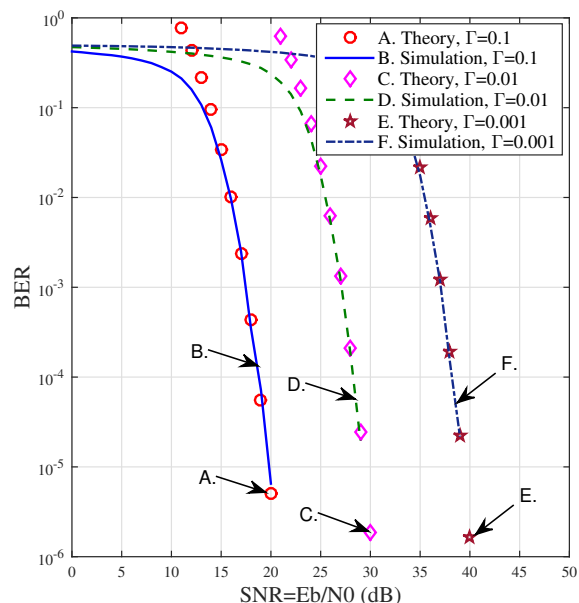


Fig. 4. Theoretical and simulation BER Performance of multi-carrier $\beta\beta^2/1$ non-binary code on additive Middleton class A noise channel for different values Γ vs. SNR in dB.

V. CONCLUSION

In this letter, the analysis of NB-convolutional codes on additive impulsive noise has been introduced. Furthermore, the theoretical bound of binary and NB-convolutional coded OFDM-PLC systems have been investigated for the first time. In order to validate our results, the implementation of simulated and theoretical results have been obtained for different values of the noise parameters and on different PLC channels. It is worth noting that the NB code's performance

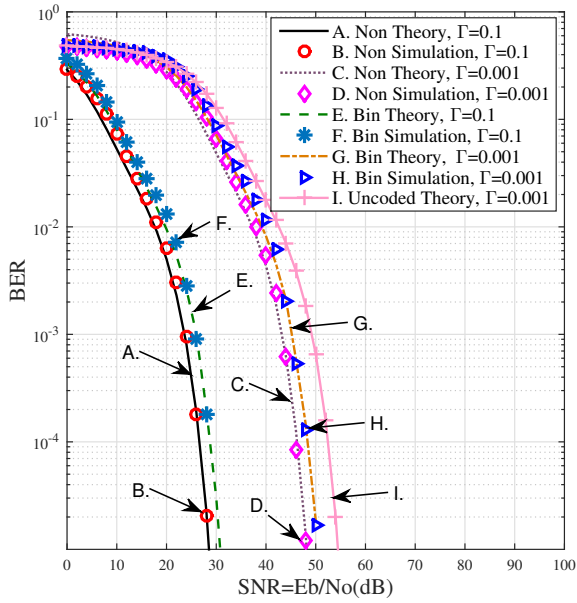


Fig. 5. BER of coded $(1, 7/5)_8$ binary and $\beta_1\beta/\beta^2/1$ NB-convolutional OFDM-PLC systems over 4 multi-path channel vs. SNR in dB.

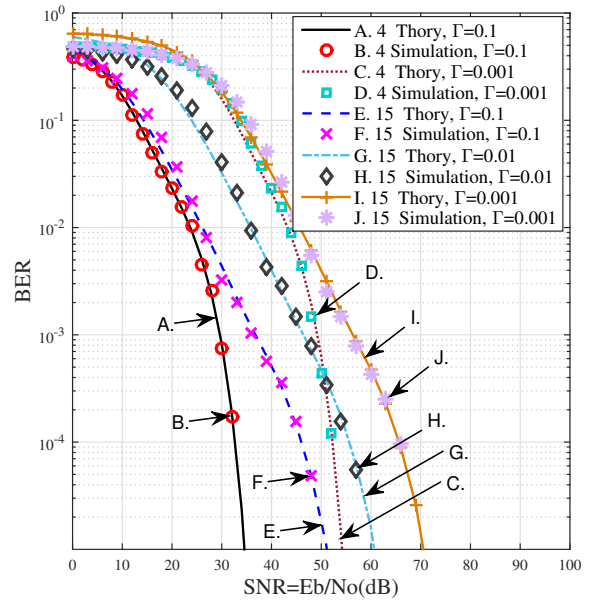


Fig. 7. BER of coded $\beta\beta^2/1$ NB-convolutional OFDM-PLC systems vs. SNR in dB.

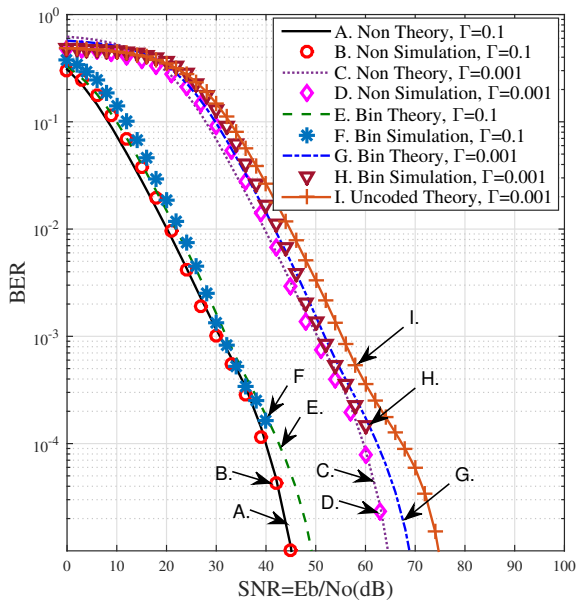


Fig. 6. BER of coded $(1, 7/5)_8$ binary and $\beta_1\beta/\beta^2/1$ NB-convolutional OFDM-PLC systems over 15 multi-path channel vs. SNR in dB.

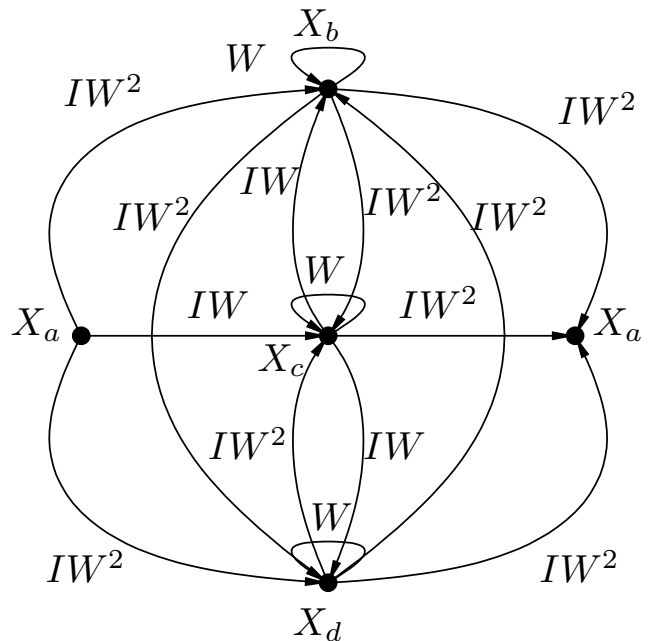


Fig. 8. The signal flow-graph of the $\beta\beta^2/1$ NB-convolutional code.

surpassed the binary code's performance in all cases. Finally, our results showed a great agreement between the simulated and theoretical analysis for all cases.

APPENDIX

DRIVING THE TRANSFER FUNCTION AND WEIGHT ENUMERATORS OF THE $\beta\beta^2/1$ NB-CONVOLUTIONAL CODE

Figure 8 presents the signal flow graph of the $\beta\beta^2/1$ NB code. Hence, the power of W is the Hamming distance between the output bits corresponding to each state transition

and the output (00). With the help of the signal flow graph, the TF can be evaluated as shown below.

X_a represents state 0, X_b stands for state 1, X_c is state β and X_d is state β^2 .

$$X_b = IW^2 X_a + W X_b + IW X_c + IW^2 X_d \quad (18)$$

$$X_c = IW X_a + IW^2 X_b + W X_c + IW^2 X_d \quad (19)$$

$$X_d = IW^2 X_a + IW^2 X_b + IW X_c + W X_d \quad (20)$$

$$X'_a = IW^2 X_b + IW^2 X_c + IW^2 X_d \quad (21)$$

By subtracting 18 from 20, it is easy to find that $X_b = X_d$, then the transfer function is

$$\begin{aligned} X_b - X_d &= (W - IW^2)X_b + (IW^2 - W)X_d \\ (1 - W + IW^2)X_b &= (1 - W + IW^2)X_d \\ \therefore X_b &= X_d. \end{aligned}$$

The transfer function $T(I, W)$ of the signal-flow-graph in figure 8 is:

$$T(I, W) = \frac{X'_a}{X_a} = \frac{2W^2X_b + WX_c}{X_a} \quad (22)$$

$$\begin{aligned} T(I, W) &= \frac{2IW^2X_b + I^2W^3X_a + I^2W^4X_b + IW^3X_c + I^2W^3X_b}{X_a} \\ &= \frac{X_b}{X_a}(2IW^2 + I^2W^4 + I^2W^3) + I^2 + W^3 + \frac{X_c}{X_a}(IW^3) \quad (23) \end{aligned}$$

We can show that

$$X_b = \frac{IW^2X_a + IWX_c}{1 - W - IW^2} \quad (24)$$

and

$$X_c = \frac{IWX_a + 2IW^2X_b}{1 - W} \quad (25)$$

Substituting X_c into X_b gives:

$$X_b = \frac{IW^2X_a}{1 - W - IW^2} + \frac{IW(IWX_a + 2IW^2X_b)}{(1 - W - IW^2)(1 - W)}$$

$$\therefore \frac{X_b}{X_a} = \frac{IW^2 - IW^3 + I^2W^2}{1 - 2W - IW^2 + W^2 + IW^3 - 2I^2W^3} \quad (26)$$

Likewise,

$$\frac{X_c}{X_a} = \frac{IW - IW^2 - I^2W^3 + 2I^2W^4}{1 - 2W - IW^2 + W^2 + IW^3 - 2I^2W^3} \quad (27)$$

By submitting 26 and 27 into 23, the transfer function can be written as:

$$T(I, W) = \frac{I^2W^3 + 2I^2W^4 + 2I^3W^4 - 2I^2W^5 - I^3W^5 + 2I^3W^6}{1 - 2W - IW^2 + W^2 + IW^3 - 2IW^3} \quad (28)$$

Evaluating 28 gives:

$$T(I, W) = I^2W^3 + 4I^2W^4 + 7I^2W^5 + \dots \quad (29)$$

Formula 29 indicates that there is one path of Hamming distance 3 symbols, four paths of distance 4 symbols and seven paths of distance 5 symbols, etc.

In order to demonstrate the accuracy of equation 6 for both binary $(1, 7/5)_8$ and NB $(\beta \beta^2/1)$ and $(\beta^1\beta/\beta^21)$ codes, T'_w for NB codes can be calculated as:

$$T'_w = \left[\frac{d}{dI} T'(I, W) \right]_{I=1} \quad (30)$$

$$T'_w = 2W^3 + 8W^4 + 14W^5 \dots \quad (31)$$

Also the $T(I, W)$ and T'_w of the $\beta^1\beta/\beta^21$ code are evaluated manually from the trellis, respectively as:

$$T(I, W) = (I^2 + I^3)W^4 + 0W^5 + (7I^3 + 4I^4)W^6 \dots \quad (32)$$

$$T'_w = 5W^4 + 0W^5 + 33W^6 \dots \quad (33)$$

While T'_w for the binary code can be found in [15]:

$$T'_w = W^5 + 4W^6 + 12W^7 \dots \quad (34)$$

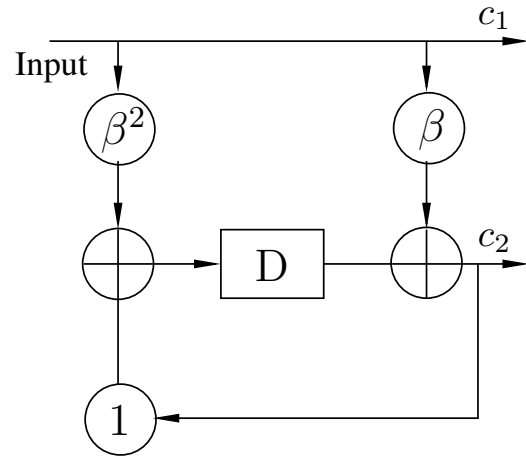


Fig. 9. $\beta \beta^2/1$ NB-convolutional encoder.

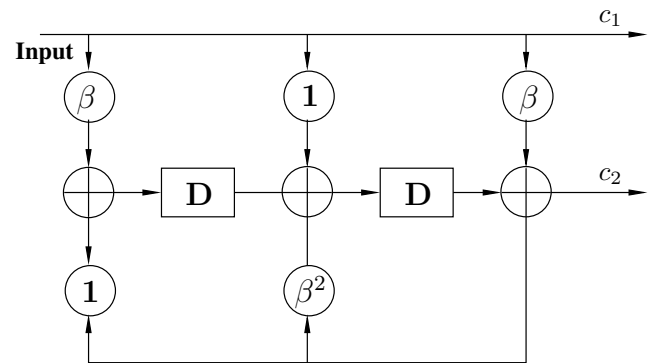


Fig. 10. $\beta^1\beta/\beta^21$ NB-convolutional encoder.

REFERENCES

- [1] D. Middleton, "Statistical-physical models of electromagnetic interference," *IEEE Transactions on Electromagnetic Compatibility*, no. 3, pp. 106–127, 1977.
- [2] A. Pittolo and A. Tonello, "A synthetic statistical mimo plc channel model applied to an in-home scenario," *IEEE Transactions on Communications*, pp. 2543–2553, 2017.
- [3] C. Hsu, N. Wang, W.-Y. Chan, and P. Jain, "Improving a power line communications standard with ldpc codes," *EURASIP Journal on Advances in Signal Processing*, vol. 2007, no. 1, pp. 1–9, 2007.
- [4] A. Hadi, K. M. Rabie, and E. Alsusa, "Polar codes based ofdm-plc systems in the presence of middleton class-a noise," in *Communication Systems, Networks and Digital Signal Processing (CSNDSP), 2016 10th International Symposium on*. IEEE, pp. 1–6, 2016.
- [5] V. Vijaykumar, P. Vanathi, P. Kanagasabapathy, and D. Ebenezer, "High density impulse noise removal using robust estimation based filter," *IAENG International Journal of Computer Science*, vol. 35, no. 3, pp. 259–266, 2008.

- [6] K. M. Rabie and E. Alsusa, "Threshold and scaling factor optimization for enhancing impulsive noise cancellation in plc systems," in *2014 IEEE Global Communications Conference*. IEEE, pp. 2977–2982, 2014.
- [7] S. Najjar, F. Rouissi, H. Gassara, A. H. Vinck, and A. Ghazel, "Novel low complexity decoding method for the binary coded frequency shift keying modulation," *Concurrency and Computation: Practice and Experience*, vol. 33, no. 1, p. e5760, 2021.
- [8] P. Agarwal and M. Shukla, "Effect of various interleavers on uncoded and coded ofdm-idma over plc," in *2020 5th International Conference on Communication and Electronics Systems (ICCES)*. IEEE, pp. 275–279, 2020.
- [9] L. Cadena, D. Castillo, A. Zotin, F. Cadena, and P. Diaz, "Evaluation of noise reduction filters in medical image processing using openmp," *IAENG International Journal of Computer Science*, vol. 46, no. 4, pp. 582-593, 2019.
- [10] R. A. Carrasco and M. Johnston, *Non-binary error control coding for wireless communication and data storage*. John Wiley & Sons, 2008.
- [11] M. Zimmermann and K. Dostert, "A multipath model for the powerline channel," *IEEE Transactions on communications*, vol. 50, no. 4, pp. 553–559, 2002.
- [12] W. Abd-Alaziz, M. Johnston, and S. Le Goff, "Non-binary turbo codes on additive impulsive noise channels," in *Communication Systems, Networks and Digital Signal Processing (CSNDSP), 2016 10th International Symposium on*. IEEE, pp. 1–5, 2016.
- [13] W. Ryan and S. Lin, *Channel codes: classical and modern*. Cambridge university press, 2009.
- [14] J. Proakis, *Digital Communications*, ser. McGraw-Hill series in electrical and computer engineering : communications and signal processing. McGraw-Hill, 2001.
- [15] P. Frenger, P. Orten, and T. Ottosson, "Convolutional codes with optimum distance spectrum," *IEEE Communications letters*, vol. 3, no. 11, pp. 317–319, 1999.